Food Chemistry 383 (2022) 132330

Contents lists available at ScienceDirect

Food Chemistry

journal homepage: www.elsevier.com/locate/foodchem

Hyaluronic acid and human/bovine serum albumin shelled nanocapsules: Interaction with mucins and *in vitro* digestibility of interfacial films

Teresa del Castillo-Santaella [a,b,1], Aixa Aguilera-Garrido [a,1], Francisco Galisteo-González [a], María José Gálvez-Ruiz [a,c], José Antonio Molina-Bolívar [c,d], Julia Maldonado-Valderrama [a,c,*]

[a] Department of Applied Physics, University of Granada, Avenida de Fuente Nueva, s/n, C.P. 18071 Granada, Spain
[b] Department of Physical Chemistry, University of Granada, Campus Universitario s/n, C.P. 1807 Granada, Spain
[c] Excellence Research Unit "Modeling Nature" (MNat), University of Granada, Avda. del Hospicio, s/n, C.P. 18010 Granada, Spain
[d] Department of Applied Physics II, Engineering School, University of Málaga, 29071 Málaga, Spain

ARTICLE INFO

Keywords:
Albumin
Hyaluronic acid
Digestion
Mucin
Emulsion
Interfacial tension

ABSTRACT

Liquid lipid nanocapsules are oil droplets surrounded by a protective shell, which enable high load and allow controlled delivery of lipophilic compounds. However, their use in food formulations requires analysing their digestibility and interaction with mucin. Here, serum albumins and hyaluronic acid shelled olive oil nanocapsules are analysed to discern differences between human and bovine variants, the latter usually used as model system. Interfacial interaction of albumins and hyaluronic acid reveals that human albumin presents limited conformational changes upon adsorption, which increase by complexation with the polysaccharide present at the interface. The latter also promotes hydrophobic interactions with mucin, especially at pH 3 and protects albumin interfacial layer under *in vitro* gastric digestion. The interfacial unfolding induced in human albumin by hyaluronic acid facilitates *in vitro* lipolysis while its limited conformational changes provide the largest protection against *in vitro* lipolysis.

1. Introduction

One of the most versatile and accessible delivery nanosystems to be implemented in food products are Liquid Lipid Nanocapsules (LLNs). LLNs are nanoemulsions formed by oil droplets, which can facilitate a high load of lipophilic molecules, surrounded by an outer polymeric or surfactant shell (Aguilera-Garrido, del Castillo-Santaella, & Galisteo-González et al., 2021; Galisteo-González et al., 2018). These colloidal/nano systems are hence fully biodegradable and biocompatible and have been applied to reduce oxidation (Li et al., 2021), and encapsulate bioactive compounds and nutrients such as curcumin (Aguilera-Garrido, del Castillo-Santaella, & Galisteo-González et al., 2021; Pan et al., 2019; Yu & Huang, 2010).

The use of albumins to build up the shell of LLNs has been reported for different food and nanomedicine applications since they are non-toxic, biocompatible, biodegradable, and non-immunogenic (Aguilera-Garrido, del Castillo-Santaella, Yang et al., 2021; del Castillo-Santaella et al., 2016; Galisteo-González et al., 2018; Kim & Shin, 2021). In addition, coating the nanoparticles with albumins can increase their circulation time in the blood, hence increasing the half-life of encapsulated compound and their bioavailability (Li et al., 2021; Luo et al., 2020). Human serum albumin (HSA) and its bovine analogous (BSA) are the most used albumins in the development of delivery systems. BSA is usually considered comparable to the human homologue HSA and used as model protein in many studies. However, they display subtle structural differences which can alter their functionality and should be considered when designing delivery systems (Aguilera-Garrido, del Castillo-Santaella, Yang et al., 2021).

At any rate, the design of food-based delivery systems for lipophobic compounds requires a careful evaluation of their physical characteristics and of the digestibility and degradation profile of encapsulated compounds. Specifically, in food products LLNs need to increase their residence time in the gastrointestinal tract to achieve high absorption ratios and similar concentration in blood to those reached by parenteral

Abbreviations: HAS, Human Serum Albumin; BSA, Bovine Serum Albumin; HA, Hyaluronic Acid; LLNs, Liquid Lipid Nanocapsules; D_H, hydrodynamic diameter; PDI, polydispersity index.

* Corresponding author.
E-mail address: julia@ugr.es (J. Maldonado-Valderrama).

[1] Shared first authorship; equal contribution to the work.

https://doi.org/10.1016/j.foodchem.2022.132330
Received 21 September 2021; Received in revised form 14 January 2022; Accepted 31 January 2022
Available online 3 February 2022

delivery systems (Luo et al., 2020; Pan et al., 2019). An important steric barrier to LLNs diffusion in food products is the presence of mucus, a viscoelastic gel where mucins play an important role on defining the cross-linked gel-like structure (Radicioni et al., 2016). Mucin fibres display nanometric spacing pores of 50–1000 nm between mucin fibres, which supports the use of nanocarriers to deliver drugs by oral administration (Wagner, Wheeler, & Ribbeck, 2018). Mucus can bind all kind of molecules and particles that reach the gastrointestinal tract via hydrophobic interactions, hydrogen bonds, or electrostatic interactions, through the charged groups of mucins (mainly sialic acid and sulphated saccharides) and the hydrophobic domains on terminal regions (Petrou & Crouzier, 2018). These interactions are influenced by the ionic strength, ionic composition, and pH of the surrounding environment (Radicioni et al., 2016). Clearly, the existence of these interactions should be considered in order to design optimal strategies for food-based delivery systems.

A strategy commonly employed to increase absorption from nanoparticles via mucosal epithelium is the addition of mucoadhesive polymers such as hyaluronic acid (HA), chitosan or high molecular weight polyethylene glycol (PEG) (Aguilera-Garrido, del Castillo-Santaella, & Galisteo-González et al., 2021; Wang et al., 2008). These hydrophilic polymers enhance the gastrointestinal stability of nanocarriers by the improvement of hydration forces (Plaza-Oliver et al., 2020). HA is a well-known non-surface active polysaccharide (Aguilera-Garrido, del Castillo-Santaella, & Galisteo-González et al., 2021; Aguilera-Garrido, del Castillo-Santaella, Yang et al., 2021). It is present in different food products such as, bone broth, soy, root vegetables, some citrus fruits and leafy greens and has been used in medicine, pharmacy, cosmetics and nutrition (Fallacara et al., 2018). HA is a polymer able to bind to different biomolecules such as proteins through specific or non-specific interactions, also showing remarkable mucoadhesive properties and used in the development of vehicles for administration of compounds through mucosal epithelium (Chen et al., 2019; Fallacara et al., 2018; Yu & Huang, 2010).

A previous work addressed the encapsulation efficiency of curcumin in BSA shelled LLNs showing an important protective effect of HA provided after *in vitro* gastric digestion (Aguilera-Garrido, del Castillo-Santaella, & Galisteo-González et al., 2021). The goal of the present study is twofold. On one hand, to investigate the interaction with mucins, which was not considered in previous digestion procedures, following a recently validated method in our lab (Aguilera-Garrido et al., 2019). On the other hand, to explore in more detail the interfacial interactions, mimicking the shell of the LLNs, with special focus on understanding the protective effect provided by HA and the slight differences provided by Human and Bovine variants. The obtained results complement previous findings demonstrating the crucial role played by interfacial events to understand and control in-vitro digestion of LLNs with application on the rational design of food-based delivery systems.

2. Materials and methods

2.1. Materials

Bovine serum albumin (BSA, CAS [9048-46-8]), human serum albumin (HSA, CAS [70024-90-7]), glutaraldehyde (GAD, CAS [111-30-8]), mucin from porcine stomach type III (CAS [84082-64-4]), pepsin from porcine gastric mucosa (P7012-1G, CAS [9001-75-6], trypsin from porcine pancreas (T0303-1G, CAS [9002-07-7]), α-chymotrypsin from bovine pancreas (C7762, CAS [9004-07-3]), lipase from porcine pancreas (L3126, CAS [9001-62-1]), sodium glycodeoxycholate (NaGDC, > 97 %, TLC, G9910, CAS [16409-34-0]), taurocholic acid sodium salt hydrate (NaTC, > 97 %, TLC, T4009, CAS [345909-26-4]) and highly refined olive oil were commercially supplied by Sigma-Aldrich® (Madrid, Spain). Sodium hyaluronate was kindly provided by Bioiberica (1982 kDa). Ethanol (analytical grade) was purchased from Merck (Madrid, Spain). Dialysis membrane (300 kDa MWCO, biotech CE membrane 131456) was purchased from Spectrum Labs (Breda, The Netherlands). For the interfacial characterisation, the olive oil was purified with Florisil® resins (Fluka, 60-10 mesh, 46385) prior to use by following the procedure used in previous works (del Castillo-Santaella et al., 2016; Maldonado-Valderrama, Holgado-Terriza, Torcello-Gómez, & Cabrerizo-Vílchez, 2013).

2.2. Preparation of LLNs

LLNs were prepared following a solvent displacement method previously described (Aguilera-Garrido, del Castillo-Santaella, & Galisteo-González et al., 2021). The organic phase was prepared by dissolving olive oil in ethanol at 0.75 % (v/v). The aqueous phase was prepared by dissolving albumin (BSA or HSA at 0.75 mg/mL) and HA (0.19 mg/mL, when needed) in ultrapure water and adjusting pH to 7.5 with NaOH. The organic and aqueous phases were mixed at a 1:1 (v/v) ratio, by injecting the organic phase into the aqueous one. After mixing, the dispersion became turbid owing to the formation of LLNs. After 10 min stirring, GAD was added (0.008 % final concentration) and stirred for 15 min more at room temperature (25 °C). The organic phase (ethanol) was evaporated at 34 °C in a rotary evaporator under vacuum. Finally, the LLNs were dialyzed in a 300 kDa pore size dialysis membrane for 48 h against 1 L of phosphate buffer (NaH_2PO_4 1.13 mM) at pH 7 at 6 °C, changing the dialysis solution twice. LLNs were stored at 6 °C until their use.

2.3. Colloidal characterization

Hydrodynamic diameter (D_H), polydispersity index (PDI), and ζ-potential of LLNs were measured by DLS using a Zetasizer Nano-ZS system (Malvern Instruments, UK). Samples were diluted 1:100 in low ionic strength buffers at pH 3 (acetic acid 13.5 mM) or pH 7 (NaH_2PO_4 1.13 mM). The ζ-potential was calculated according to the Smoluchowsky theory. All measurements were repeated three times for different samples and data appears as the mean value ± standard deviation.

2.4. Interaction with mucin

The interaction of LLNs with mucin was studied by recording the ζ-potential of LLNs incubated with different mucin concentrations (0–1 mg/mL) after 30 min of incubation as provided in a validated protocol (Aguilera-Garrido et al., 2019). The ζ-potential of the LLNs before and after the incubation with mucin was recorded upon dilution with the previously mentioned buffers at pH 3 or pH 7 (50 μL of LLNs solution in 1 mL of buffer). ζ-potential of LLNs were determined by Dynamic Light Scattering (DLS) using a Zetasizer Nano-ZS system (Malvern Instruments, UK). All measurements were repeated three times for different samples.

2.5. Interfacial characterization and in vitro digestion of interfacial layers

The interfacial characterization was carried out using the OCTOPUS, a Surface Film Balance equipped with a multi-subphase exchange device which has been fully designed and developed at the University of Granada and is described in detail elsewhere (Maldonado-Valderrama, Torcello-Gómez, del Castillo-Santaella, Holgado-Terriza, & Cabrerizo-Vílchez, 2015). The detection and calculation of the interfacial area (A) and the interfacial tension (γ) are based on axisymmetric drop shape analysis (ADSA) and the whole set up is computer-controlled by software packages DINATEN® and CONTACTO®. A solution droplet (approximately 10 μL of volume) is formed at the tip of a capillary, which is submerged in purified olive oil (4 mL) contained in a glass cuvette (Hellma®), located in a thermostatically controlled cell. The interfacial tension is measured in real time at constant area (20 mm^2) every each second during the first 300 s of the adsorption and then, each 5 s for approximately 1 h. Once a stable layer is formed, i.e., interfacial

tension remains unchanged, the dilatational modulus (E) of the adsorbed layer is measured by oscillating the drop volume. The E is obtained by applying volume oscillations at amplitude values of<5 %, to avoid excessive perturbation of the interfacial layer, and at an oscillation frequency of 0.1 Hz. The obtained E is a complex magnitude accounting for the interfacial elasticity and viscosity of the interfacial layer but at this frequency, the dilatational response is mainly elastic, and the viscous component can be neglected (Maldonado-Valderrama, Muros-Cobos, Holgado-Terriza, & Cabrerizo-Vílchez, 2014; Maldonado-Valderrama et al., 2015).

The OCTOPUS allows to exchange the bulk of the drop maintaining the interfacial area constant. This accessory is applied to measure sequential adsorption of albumins and HA. In a first step, the protein absorbs on to the oil–water interface and after equilibration the E is measured. Then, the bulk protein solution is exchanged by a HA solution ($7{\cdot}10^{-5}$ M) allowing sequential adsorption to proceed. The interfacial tension is recorded throughout the whole subphase exchange process and the E is measured after equilibration of the interfacial film. All the measurements are made at 37 °C.

A similar procedure is used to simulate digestion in a single droplet. The OCTOPUS allows to monitor the interfacial changes promoted by *in vitro* digestion of interfacial layers as fully described elsewhere (Aguilera-Garrido, del Castillo-Santaella, & Galisteo-González et al., 2021; del Castillo-Santaella et al., 2016; Maldonado-Valderrama et al., 2015). The interfacial layer is subjected sequentially to different digestive media by subphase exchange of the droplet bulk solution with digestive fluids. Herein, the simulated *in vitro* digestion was set in three sequential steps simulating the passage along the stomach and small intestine: pepsinolysis, trypsin/chymotrypsin proteolysis, and lipolysis. The interfacial tension is measured *in situ* along the whole digestion process and the E is measured at the end of each adsorption step. All measurements were performed at 37 °C and were repeated at least three times for different samples.

Digestive buffers were adapted from INFOGEST 1.0 harmonized protocol (Minekus et al., 2014) The digestion of interfacial layers stands as a model for digestion of emulsion by simulating digestion in a single droplet. In this way, the reduced amount of sample requires the use of a simplified buffer to prevent the presence of surface-active impurities or agents that may hinder interfacial effects. The characteristics of the experimental device require the use of simplified buffers solutions, and the drop volume makes necessary to adapt slightly enzymes activities, bile salts concentrations and electrolyte as we have used and validated in previous publications works (Aguilera-Garrido, del Castillo-Santaella, & Galisteo-González et al., 2021; Maldonado-Valderrama et al., 2013; Maldonado-Valderrama et al., 2015). Simplified Simulated Gastric Fluid (sSGF, NaH_2PO_4 1.13 mM, NaCl 150 mM at pH 3), and simplified Simulated Intestinal Fluid (sSIF NaH_2PO_4 1.13 mM, NaCl 150 mM, $CaCl_2$ 3 mM and pH 7). Pepsin (1 U/mg substrate) was freshly prepared in sSGF. Trypsin (0.12 U/mg substrate), chymotrypsin (0.24 U/mg substrate), lipase (0.16 mg/mL, 69 U/mg susbtrate) and bile salts (1 mM, 52.7 % NaTC and 47.3 % NaGDC) were freshly prepared in sSIF. Enzymes were prepared immediately before use, and stored in ice until use, to avoid enzyme autolysis. The interfacial tension of the purified olive oil–water interface was measured before every experiment, in order to confirm the absence of surface-active contaminants, yielding values of 29.5 ± 0.5 mN/m at 20 °C.

2.6. Statistical analysis

Statgraphics 18 (Statistical Graphics Corp., Rockville, MD, USA) free version was used for statistical data analysis. All data are expressed as mean ± standard deviation. First, ANOVA was assayed with p-value < 0.001, followed by performance of Tukeýs multiple sample comparison analysis to identify significant differences between data. Differences between mean values were considered significant at a level of confidence of 95 % ($p < 0.05$).

3. Results and discussion

3.1. Colloidal characterization of albumins and albumins + HA LLNs

LLNs stabilised by BSA, HSA, HA, BSA + HA, or HSA + HA were prepared and characterized by DLS to study the interactions in the shell. Table 1 shows the D_H and the ζ-potential of LLNs measured at pH 7 and pH 3.

At pH 7, all LLNs display a similar D_H with values around 150 nm (Table 1), in agreement with similar LLNs (Aguilera-Garrido, del Castillo-Santaella, & Galisteo-González et al., 2021; Aguilera-Garrido, del Castillo-Santaella, Yang et al., 2021; del Castillo-Santaella et al., 2016). Those containing only albumins or albumins + HA are monodispersed at pH 7 and remain stable over time for 2–3 months. HA is also able to form and stabilise LLNs at pH 7, but the resulting system is only stable for 1 week (data not shown). BSA-shelled LLNs appear slightly smaller than HSA or HA-shelled LLNs, whereas albumins + HA-shelled LLNs display a similar size according to statistics (p-value < 0.05). Differently, at pH 3, the size and stability of LLNs varies strongly with the composition of the shell (Table 1). The D_H of BSA-shelled LLNs appears again smaller than HSA-shelled LLNs and both form stable emulsions according to their size and polydispersity index. The D_H of BSA + HA-shelled LLNs increases significantly, though the system remains stable. Conversely, LLNs composed of HA or HSA + HA appear aggregated at pH 3 as their polydispersity index increases over 0.25.

The ζ-potential of LLNs also depends on pH, providing information on the surface composition of LLNs. On the one hand, at pH 7, all LLNs show a similar negative value without significant differences according to the statistical study (Table 1). Indeed, at this pH, the carboxylic groups are negatively charged, while amino groups offer practically no charge. On the other hand, at pH 3, the measured ζ-potential of LLNs varies with the composition of the shell. LLNs composed of BSA or HSA display a positive charge due to the protonation of carboxylic and amine groups below their isoelectric point. Besides, LLNs composed of mixtures, namely BSA + HA or HSA + HA, show a positive ζ-potential at pH

Table 1
Average droplet D_H and ζ-potential of different LLNs measured at pH 7 buffer (NaH_2PO_4 1.13 mM) and pH 3 buffer (acetic acid 13.5 mM). All the measurements were performed at 25 °C and the results were obtained from the average value of three different synthesis. Data appear as the mean value ± standard deviation. The one-way ANOVA with post-hoc Tukeýs statistical study assigned different letters (a, b-d, o-s and x-y) which indicate significant differences ($p < 0.05$).

	pH 7			pH 3		
LLNs	D_H (nm)	PDI	ζ-potential (mV)	D_H (nm)	PDI	ζ-potential (mV)
BSA	144 ± 5^{x}	0.15 ± 0.07	$-(37 \pm 7)^{a}$	158 ± 5^{o}	0.03 ± 0.02	55 ± 6^{b}
BSA + HA	$156 \pm 10^{x,y}$	0.11 ± 0.04	$-(39 \pm 6)^{a}$	311 ± 10^{p}	0.24 ± 0.07	30 ± 5^{c}
HA	168 ± 11^{y}	0.08 ± 0.02	$-(35 \pm 9)^{a}$	1940 ± 60^{q}	0.78 ± 0.08	$-(12.3 \pm 1.1)^{d}$
HSA	172 ± 11^{y}	0.13 ± 0.05	$-(34 \pm 7)^{a}$	180 ± 8^{r}	0.05 ± 0.01	54.7 ± 1.1^{b}
HSA + HA	$156 \pm 16^{x,y}$	0.14 ± 0.05	$-(34 \pm 10)^{a}$	756 ± 30^{s}	0.52 ± 0.14	25 ± 3^{c}

3, but significantly lower than that of HSA or BSA LLNs (Table 1, p-value < 0.05). This could be due to the inclusion of negatively charged HA within the shell of the LLNs for both albumins, although not with enough extension to overturn the net positive charge into negative values, as observed in the case of HA LLNs. According to Moore and Cerasoli, when the ζ-potential values are below −30 mV or above +30 mV, the electrostatic repulsion is high enough to avoid physical destabilization (Moore & Cerasoli, 2017). The characteristics of LLNs displayed in Table 1 agree with this fact. At pH 7 all LLNs show negative charges above 30 mV (in absolute value) and are colloidally stable. Conversely, at pH 3, LLNs displaying ζ-potential values in the range [–30 mV, + 30 mV] are unstable, namely HA and HSA-HA LLNs (Table 1).

LLNs stabilised solely by HA are remarkably interesting systems, showing negative ζ-potential at pH 3 and pH 7 (Table 1). This negative value is due to the low isoelectric point of HA (pH 2.5), a molecule negatively charged due to the carboxylic groups located on its glucuronic acid moieties, which also contribute to the molecule stabilization through hydrogen bonds (Fallacara et al., 2018). Despite HA being non-surface active, HA is able to stabilise LLNs which remain stable for a few days. There are some other examples in the literature of non, or low, surface active molecules with high viscosity used to stabilize emulsions, such as Acyl Gellan Gum (Lorenzo, Zaritzky, & Califano, 2013) and hydrophobically–hydrophilically modified Hydroxyethylcellulose (Akiyama et al., 2005). The existence of stable HA-shelled LLNs is possibly due to steric stabilisation and thickening of the continuous phase owing to the high viscosity of HA solutions, which originates from its high molecular weight and the semi-flexibility of the chains. Furthermore, Uspenskii et al. showed that the viscosity of HA solutions depends strongly on pH. At pH 3.5, HA chains adopt a compact conformation with reduced viscosity. The negative charge of the molecule increases as the pH rises, leading to a less compact and more interconnected structure with higher thickening abilities, which provides a more viscous continuous phase (Uspenskii, Kil'deeva, Maslova, Demina, & Vikhoreva, 2016). Accordingly, at pH 7 the higher viscosity of HA solutions will allow oil droplets to remain as individuals HA-shelled LLNs, while the reduced viscosity of HA solutions at pH 3 may promote coalescence of LLNs. This would agree with the data shown in Table 1, where stable HA LLNs are observed at pH 7, but they appear aggregated at pH 3, according to their size and polydispersity index.

3.2. Interaction of LLNs with mucins: Effect of HA

Mucin interacts with different kind of molecules, and the absorption through the digestive tract will be improved or not depending on these interactions as it influences drug diffusivity through mucosal epithelium (Plaza-Oliver et al., 2020) Still, mucins are not generally included in digestive buffers, according to international standard protocols developed by INFOGEST. Hence, the interaction with mucins was measured in a separate experiment applying gastrointestinal conditions following a previously described and validated method (Aguilera-Garrido et al., 2019). Interaction with oral mucins omitted here, given the reduced time that an emulsion would spend in the mouth compared to gastric and intestinal phase. Ionic strength and temperature were fixed to physiological ratios and the effect of pH, which changes from neutral to acid to neutral again during the gastrointestinal digestion process was analysed. Hence, changes on the ζ-potential of the LLNs after incubation at pH 7 with different mucin concentrations have been evaluated at pH 3 and pH 7, matching stomach and intestinal pH, respectively.

Fig. 1 shows the ζ-potential of the different LLNs as a function of mucin concentration at pHs 7 (Fig. 1A) and 3 (Fig. 1B). As a reference, the ζ-potential of mucin was also measured at 0.03 mg/mL, obtaining – (13.9 ± 0.6) mV at pH 7, and – (1.2 ± 0.6) mV at pH 3, in accordance with the accepted range of isoelectric points of mucins (between 2 and 3) (Yakubov, Papagiannopoulos, Rat, & Waigh, 2007).

Fig. 1 shows that the ζ-potential of HA-shelled LLNs with mucin changes steeply to a less negative value as soon as a minimum concentration of mucin is present in the solution (0.05 mg/mL) at pHs 7 and 3 (Fig. 1). At pH 7, the ζ-potential reaches a plateau of ca. – 9 mV above mucin concentration of 0.25 mg/mL. Conversely, at pH 3 the ζ-potential of HA-LLNs change to values close to 0 mV (from −0.13 ± 0.14 mV to 0.86 ± 0.09 mV) even with the minimum mucin concentration assayed. Mucin and LLNs present a net negative charge at pH 7 and samples were diluted 20 times with the appropriate buffer to study their electrokinetic properties, therefore, these data suggest that mucin interacts strongly with HA-shelled LLNs at pH 7. The changes observed on the ζ-potential may then be ascribed to the formation of a stable and irreversibly bound mucin layer around the LLNs (Aguilera-Garrido et al., 2019), with hydrogen bonding as the main driving force (Hansen et al., 2017). Nevertheless, hydrophobic interaction could also play a role in this system, since mucin possess hydrophobic domains in the terminal regions that could interact with hydrophobic patches in the shells.

It is important to note that the plateau value of ζ-potential reached by HA LLNs at pH 7 (ca. – 9 mV) is lower (in absolute values) than the ζ-potential of mucin in solution at pH 7, – (13.9 ± 0.6) mV. In the case of pH 3, the plateau value is ca. 0 mV, while the ζ-potential of mucin in solution is – (1.2 ± 0.6) mV. These low values, may be related to the conformation of adsorbed mucin at the surface of these LLNs. If we assume that the hydrophobic domains at the terminal regions of mucin can interact with the surface of the LLNs, it would lead to a conformation of

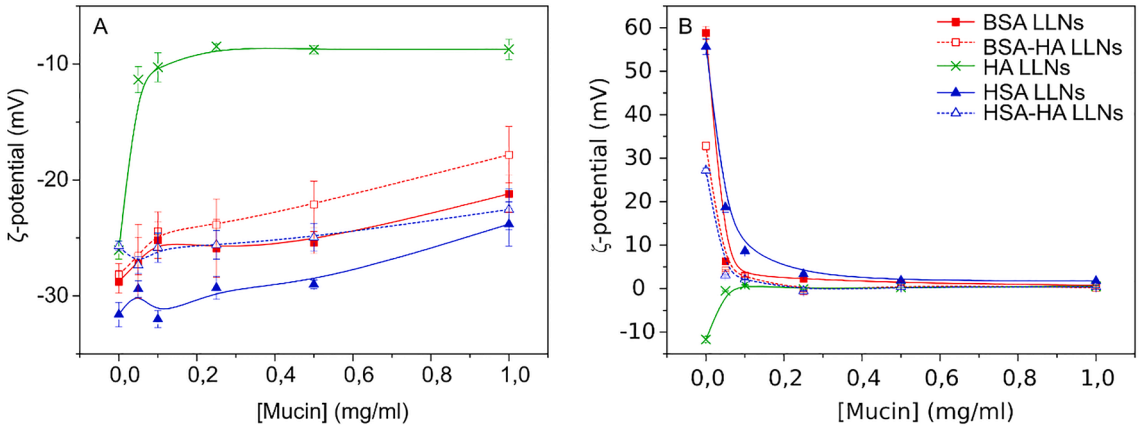

Fig. 1. ζ-Potential at (A) pH 7 and (B) pH 3 for BSA LLNs (red solid squares and solid lines), BSA-HA LLNs (red hollow squares and dashed lines), HA LLNs (green solid crosses and solid lines), HSA LLNs (blue solid triangles and solid lines) and HSA-HA LLNs (blue hollow triangles and dashed lines) with different mucin concentrations (0, 0.05, 0.1, 0.25, 0.5 and 1 mg/mL). Plotted values are mean ± standard deviation. (For interpretation of the references to colour in this figure legend, the reader is referred to the web version of this article.)

adsorbed mucin with these terminal regions attached to the LLNs, while the hydrophilic glycosylated central region would orientate towards the aqueous medium (Yakubov et al., 2007). Moreover, the polysaccharides on the central region from mucins might be also interacting with the HA at the surface of LLNs. Therefore, the adsorption of mucin onto the surface of HA-shelled LLNs may hinder some charges of mucin, providing the slightly lower ζ-potential of mucin + HA-shelled LLNs compared with the ζ-potential of pure mucin in solution.

Consider now the interactions of mucin with albumin and albumin + HA-shelled LLNs (Fig. 1). At pH 3 (Fig. 1B), the four LLNs display a drastic reduction of the ζ-potential upon interaction with the minimum mucin concentration assayed. However, at pH 7, the exposure of LLNs with mucin does not provoke such a substantial variation. In the case of BSA and BSA + HA-shelled LLNs, the ζ-potential decreases (in absolute values) up to a mucin concentration of 0.1 mg/mL, and above this concentration, the slope decreases. However, in the case of HSA and HSA + HA-shelled LLNs, the ζ-potential remains practically unchanged and just decreases at the highest concentrations of mucin.

The data obtained at pH 3 (Fig. 1B) show clearly that mucin adsorbs onto the four types of LLNs while results at pH 7 (Fig. 1A) show a weaker interaction between LLNs and mucin. There are two possible explanations to the different behaviour encountered. On one hand, at pH 7 mucin adsorbs onto LLNs overcoming the repulsive electrostatic interaction, but in a weak and reversible form. Then, upon dilution in a buffer with this same pH, mucin detaches from the particles. However, upon dilution with a pH 3 buffer, changes the repulsive electrostatic interaction to attractive, thus preventing desorption of mucin from LLNs. Another option could be that at pH 7 mucin barely adsorbs onto LLNs owing to the repulsive electrostatic interaction. Then, upon dilution with a pH 3 buffer, and despite the reduction in mucin concentration, the now attractive interaction promotes the binding of dissolved mucin molecules onto LLNs, even at the lower concentrations employed, so as to alter drastically the electrokinetic behaviour of the LLNs. Results from Fig. 1 demonstrate the existence of an attractive interaction between mucin and LLNs at pH 7, although seemingly weak. This result could favour the diffusivity of LLNs through the mucus, since it favours the interaction with the intestinal mucus but avoids an excessive binding, which could hinder nanoparticles from reaching the epithelium. Taking into account that electrostatic forces at pH 7 are repulsive, the driving forces for this interaction should come from hydrogen bonds between hydroxyl and carboxyl groups from HA and/or albumins, and glycosyl groups from mucin (Hansen et al., 2017), and hydrophobic interaction of the hydrophobic domains of mucin with the hydrophobic surface of LLNs (Yakubov et al., 2007) or the hydrophobic sites of albumins (Aguilera-Garrido, del Castillo-Santaella, Yang et al., 2021).

There are some literature studies dealing with the interaction of mucin with albumins or other polysaccharides that can provide more information on this matter. List et al. studied the interaction of mucin with serum albumins by analysing changes on the viscosity of solutions containing mucin, albumins, and mucin-albumin mixtures, at different pHs (from 7 to 9) and at different ionic strengths. Therein, the increased viscosity of the mixtures solutions was ascribed to the interaction between mucins and albumins. According to List et al. the main force involved in this interaction is the hydrophobic, with some contribution of hydrogen bonds (List, Findlay, Forstner, & Forstner, 1978). On the other hand, de Olivera-Cardoso et al., studied the mucoadhesive properties of anionic polysaccharide gellan gum with mucin obtaining a stronger interaction at an acidic pH 1.2 compared to neutral pH 6.8, mimicking the pH gradient on the gastrointestinal tract (de Oliveira Cardoso et al., 2020). At pH 6.8, the highly negative charge of both interacting molecules hindered the hydrophobic interaction and the formation of hydrogen bonds. In contrast, at pH 1.2 the carboxyl groups of mucins and gellan gum were protonated and lost their negative charge, which led to the reduction of the electrostatic repulsive forces between the molecules, allowing the formation of hydrogen bonds and Van der Walls interactions. This importantly agrees with findings and interpretation of Fig. 1.

It is also remarkable the stronger interaction with mucin obtained for HA-LLNs compared to albumin + HA-LLNs (described above and reflected in Fig. 1). This finding suggests a different conformation or positioning of the HA molecules at the surface of LLNs when albumin is present, in such a way that numerous hydroxyl and carboxyl groups from HA, which have the potential to establish hydrogen bonds with mucin, are hidden. Another interesting finding deduced from Fig. 1A is the different interaction pattern observed between BSA- and HSA- LLNs: despite the similarity of these albumins, they show different mucoadhesive properties. The origins are possibly related to the slight differences in the molecular structure of both albumins and their interfacial conformation at the oil–water interface. This is an important issue to consider in the indistinct use of these proteins in delivery systems. Structural differences between BSA and HSA (recently reviewed by (Aguilera-Garrido, del Castillo-Santaella, Yang et al., 2021) can originate slight differences in terms of interacting abilities with other molecules and in terms of stability. Some of these will be analysed in more detail in the next section.

3.3. Interaction of HA and albumins at oil–water interface

To further understand the different behaviour and interacting abilities found with HSA and BSA covered LLNs, this section investigates their interfacial characteristics. The conformational changes of proteins upon adsorption at an interface are reflected in changes of interfacial tension and dilatational viscoelasticity (del Castillo-Santaella et al., 2016; Maldonado-Valderrama et al., 2015). Albumins present polar and apolar regions in their globular conformation which are exposed onto the oil–water interface upon adsorption changing their conformation depending on thermodynamic stability, flexibility, amphipathicity, molecular size and charge of protein molecules.

Fig. 2A shows the final interfacial tension (γ) attained after 1 h of adsorption onto the olive oil–water interface for different concentrations of BSA and HSA. In agreement with other studies (del Castillo-Santaella et al., 2016), the final interfacial tension decreases as the concentration of protein increases in the bulk, until it reaches a plateau when the interfacial layer reaches maximum interfacial coverage, as shown in Fig. 2A. The final interfacial tension of BSA appears significantly lower than that of HSA, suggesting a higher interfacial coverage of the BSA adsorbed layer. This is more noticeable at the lowest studied concentrations. According to these findings, BSA seems to be more surface active than HSA, as previously reported in literature (Lu, Su, & Penfold, 1999). This also correlates with other experimental results showing that BSA forms a more extended monolayer, owing to a loss of tertiary structure upon adsorption that enables an improved interfacial coverage (Ma, Ferhan, Sut, Jackman, & Cho, 2020). In fact, according to Douillard, interfacial unfolding of BSA is improved at oil–water compared to air–water interfaces, and this fact agrees with the higher interfacial coverage inferred from Fig. 2A (Douillard, 1994).

Fig. 2B shows the dilatational elastic modulus or interfacial elasticity (E) of the interfacial layer formed by HSA and BSA after 1 h of adsorption onto the oil–water interface. This magnitude provides information about intra- and intermolecular interactions within the interfacial layer (Maldonado-Valderrama et al., 2014). Fig. 2B shows one single maximum for HSA and BSA adsorbed at olive oil–water interface, which is indicative of one single conformational transition existing at the interface. Moreover, E appears significantly lower for BSA within all the range of concentrations evaluated. This lower range of values relates to the lower conformational stability of BSA and HSA upon adsorption at the oil–water interface. Differences on the amino acid sequences between BSA and HSA makes HSA a more stable protein, which resist better temperature-induced and adsorption-induced unfolding (Ma et al., 2020). Therefore, the higher E of interfacial HSA reflects a less interfacial unfolding degree, which in turn provides a more cohesive and compact monolayer at the interface compared to BSA

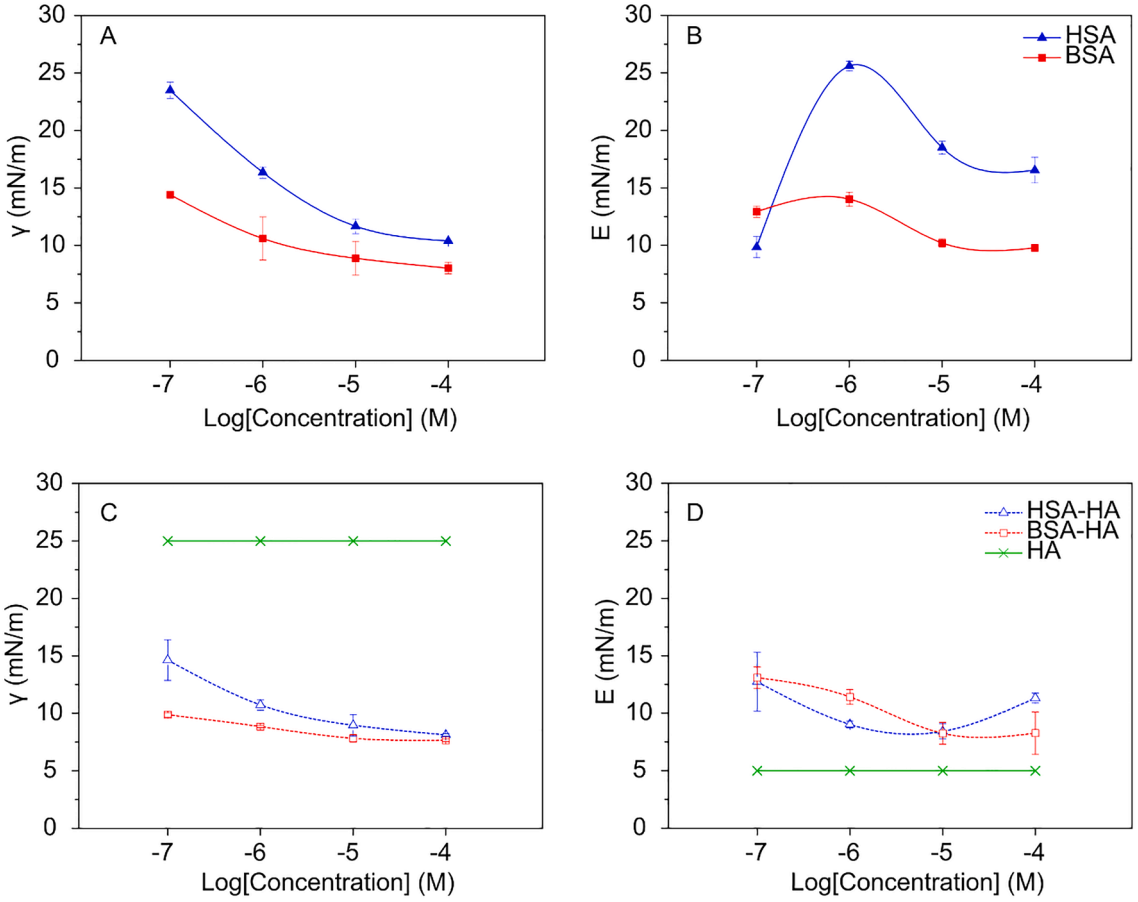

Fig. 2. (A) Interfacial tension and (B) Interfacial dilatational modulus (0.1 Hz) as a function of concentration of BSA (red solid squares) and HSA (blue solid triangles). (C) Interfacial tension and (D) Interfacial dilatational modulus (0.1 Hz) as a function of concentration of BSA + HA (red open squares) and HSA + HA (blue open triangles). Concentration of HA (green solid crosses) fixed as $5{\cdot}10^{-7}$ M. Final values reached after 1 h of adsorption at the olive oil–water interface in NaH_2PO_4 1.13 mM, pH 7.0, T = 37 ℃. Values plotted are mean values ± standard deviations (within the size of the symbols). Lines are a guide for the eye. (For interpretation of the references to colour in this figure legend, the reader is referred to the web version of this article.)

(Fig. 2B). This also agrees with the lower interfacial tension obtained for BSA; as the increased unfolding provides improved interfacial coverage because the number of interfacial anchoring points increases. Furthermore, various authors have studied the interfacial characteristics of BSA at air–water and oil–water interfaces, showing that BSA changes secondary structure and lose tertiary structure enhancing the interfacial packing of molecules (Douillard, 1994). Interfacial conformation of proteins can also play a role in emulsification. Day et al. compared abilities of BSA and lysozyme as emulsifiers, determining that BSA performs better than lysozyme owing to the freedom on the conformation rearrangement at the interface (Day et al., 2014). In a similar way, BSA will be a better emulsifier than HSA, considering the more extensive conformational changes proposed for the former. This concurs with the smaller droplet size obtained for BSA- compared to HSA-covered LLNs (Table 1).

The interfacial interaction of BSA and HSA with HA, is addressed similarly by means of interfacial tension (Fig. 2C) and E (Fig. 2D) of mixed adsorbed layers. HA shows no interfacial activity (interfacial tension ≈ 25 mN/m) as previously reported (Aguilera-Garrido, del Castillo-Santaella, Yang et al., 2021), and no elastic response (E < 5 mN/m) at the olive oil–water interface within the range of concentrations assayed. However, addition of HA improves the interfacial activity of BSA and HSA (Fig. 2C) as demonstrated by the lower interfacial tension attained by BSA + HA and HSA + HA mixtures (Fig. 2C) compared to BSA and HSA (Fig. 2A) for all the protein concentrations assayed. This improvement is more notable for HSA, making the adsorbed layer of HSA + HA comparable to that of BSA (Fig. 2A and 2C). Similarly, the E of HSA + HA adsorbed layer (Fig. 2D) reduces with respect to that of native HSA adsorbed layer (Fig. 2 B) for all the concentrations assayed. This possibly implies that interaction with HA promotes interfacial conformational changes in adsorbed HSA. Nevertheless, in the case of BSA + HA adsorbed layer, the E remains practically unchanged (Fig. 2D and 2B). This agrees with the similar size obtained for both albumins + HA LLNs (Table 1).

Murray et al. explained that adsorbed proteins and non-surface-active polysaccharides, such as HA, can affect their interfacial rheology owing to interactions of these polysaccharides with the proteins (Murray, 2011). Furthermore, these interactions can increase the thickness of the adsorbed film, which in turn alter rheological properties of the adsorbed layer (Murray, 2011). Rodríguez-Patino and Pilosof state that the effect of non-surface-active polysaccharides on proteins fluid interfaces derives from their complexation or exclusion volume effects (Rodríguez Patino & Pilosof, 2011). The complexation of albumins and HA could occur via two types of interactions. On one hand, albumins and HA may interact in the bulk or at the interface by weak electrostatic interactions, between negatively charged groups of HA and positively charged patches in HSA and BSA. The strength of this interaction depends on the charge density of the polysaccharide and the accessibility of positive patches in the protein structure (Rodríguez Patino & Pilosof, 2011). On the other hand, the interaction can take place by hydrogen bonds, also dependant on the accessibility of hydrogen bonding sites. Results shown in Fig. 2B and 2D for HSA agree with findings from Baeza et al. for β-lactoglobulin films in the presence of xanthan gum (non-surface active). They also observed a strong

increase of surface pressure, analogue to the decrease of interfacial tension recorded in Fig. 2C, accompanied by a decrease in the E, suggesting that the interaction between protein and polysaccharide weakens the protein network by a complexation mechanism or indirectly by exclusion volume effect (Baeza et al., 2006). The smaller effect of HA on the interfacial properties of BSA, interfacial tension (Fig. 2C) and especially, E (Fig. 2D), compared to HSA, could be attributed to a lower degree of complexation or lesser exclusion volume effect. These, evidence the existence of a different interaction between HA and both albumins, based on different number of hydrogen binging sites or weak positive patches with act as interacting sites for HA.

The location of HA in the interfacial layer has been further assessed by measuring the differences between competitive and sequentially adsorbed layers (Fig. 3). Competitive adsorbed layers mimic the formation of mixed shells of LLNs while in the sequential adsorption experiment, the polymer is added after the formation of a pure albumin layer by using the subphase exchange technique. Fig. 3 shows how sequential adsorption of HA onto albumin preformed layer does not show any statistically significant alterations of the interfacial tension with respect to HSA and BSA interfacial layers, suggesting that the HA does not alter the interfacial coverage. However, addition of HA does significantly increase the E of BSA and HSA interfacial layers indicative of promoted interfacial interconnections, possibly caused by the presence of HA anchored in a second layer below the interfacial film. Conversely, the lower interfacial tension of the mixed HA + albumin layer formed by competitive adsorption suggests that the HA is integrated in the interfacial film also preventing the formation of interconnections and hence reducing E (Fig. 3). These results demonstrate the formation of different interfacial films depending on the method of formation (see schematic diagram at the top of Fig. 3). Moreover, this experiment possibly demonstrates the presence of HA inserted into the protein shell of mixed LLNs. The higher interfacial tension and E obtained for sequentially adsorbed HA and HSA compared to BSA also confirms the lower conformation changes of HSA upon adsorption.

3.4. *In vitro digestion of albumins at oil–water interface: Effect of HA*

This final section analyses the effects of digestive media and enzymes on interfacial layers formed by albumins and albumins + HA. These experiments mimic the digestion of LLNs in a single droplet to focus on the gastric and intestinal digestion and investigate the protective effect of HA found in a previous work (Aguilera-Garrido, del Castillo-Santaella, & Galisteo-González et al., 2021). Fig. 4 show the effect of the sequential digestive protocol performed in a single droplet covered by a preformed interfacial layer of albumins or albumins + HA, respectively. The *in vitro* digestion of the interfacial layer was set in three sequential steps: pepsinolysis, trypsinolysis and lipolysis, mimicking the passage along the stomach and small intestine (Aguilera-Garrido, del Castillo-Santaella, & Galisteo-González et al., 2021; del Castillo-Santaella et al., 2016; Maldonado-Valderrama, 2019; Maldonado-Valderrama et al., 2013; Maldonado-Valderrama et al., 2015). The value of interfacial tension reached at the end of each digestive step is plotted in Fig. 4A and 4B and dynamic evolution of interfacial tension is measured *in situ* throughout the complete experiment (Fig. 4C and 4D).

The initial protein layer is formed in the first phase of the experimental protocol, where the protein, BSA or HSA with or without HA, dissolves in the initial buffer solution and adsorbs irreversibly at the oil–water for 1 h, at constant interfacial area. The adsorption process proceeds showing a rapid reduction of the interfacial tension and then, a slower kinetics until reaching a plateau. In general, the presence of HA accelerates the kinetics. These results agree with previously discussed results from Fig. 2A and 2C.

After the initial layer stabilises, the bulk solution is exchanged with sSGF buffer containing pepsin, and incubated for 1 h, simulating the gastric digestion (Fig. 4). The proteolysis of adsorbed proteins can cause an increase of the interfacial tension (Maldonado-Valderrama, 2019) as reported for other proteins such as β-lactoglobulin (del Castillo-Santaella et al., 2014; Maldonado-Valderrama et al., 2013) and β-casein (Maldonado-Valderrama et al., 2013) in similar digestive conditions. In the case of albumins, the interfacial tension increases owing

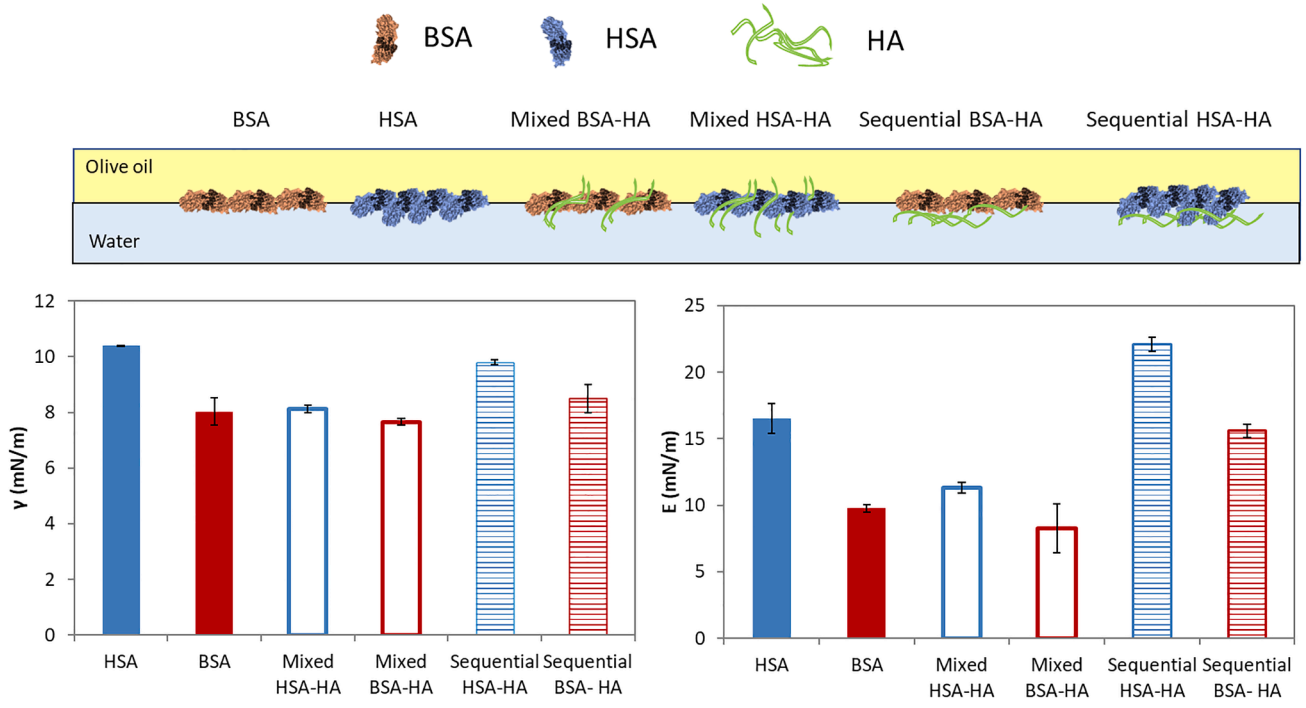

Fig. 3. The disposition of adsorbed protein HSA, BSA, mixed HSA-HA, mixed BSA-HA, sequential HSA-HA, and sequential BSA-HA at olive oil–water interface are represented according to interfacial results. After 60 min of adsorption, the final interfacial tension attained and elasticity at the 0.1 Hz of frequency of HSA, BSA, mixed HSA-HA and BSA-HA and sequential HSA-HA and BSA and BSA-HA are represented. Measurements are made at the olive oil–water interface in NaH_2PO_4 1.13 mM, pH 7.0, T = 37 ℃, concentration of HA 5·10-7 M. Different letters (a-g) indicate significant differences between samples ($p < 0.05$).

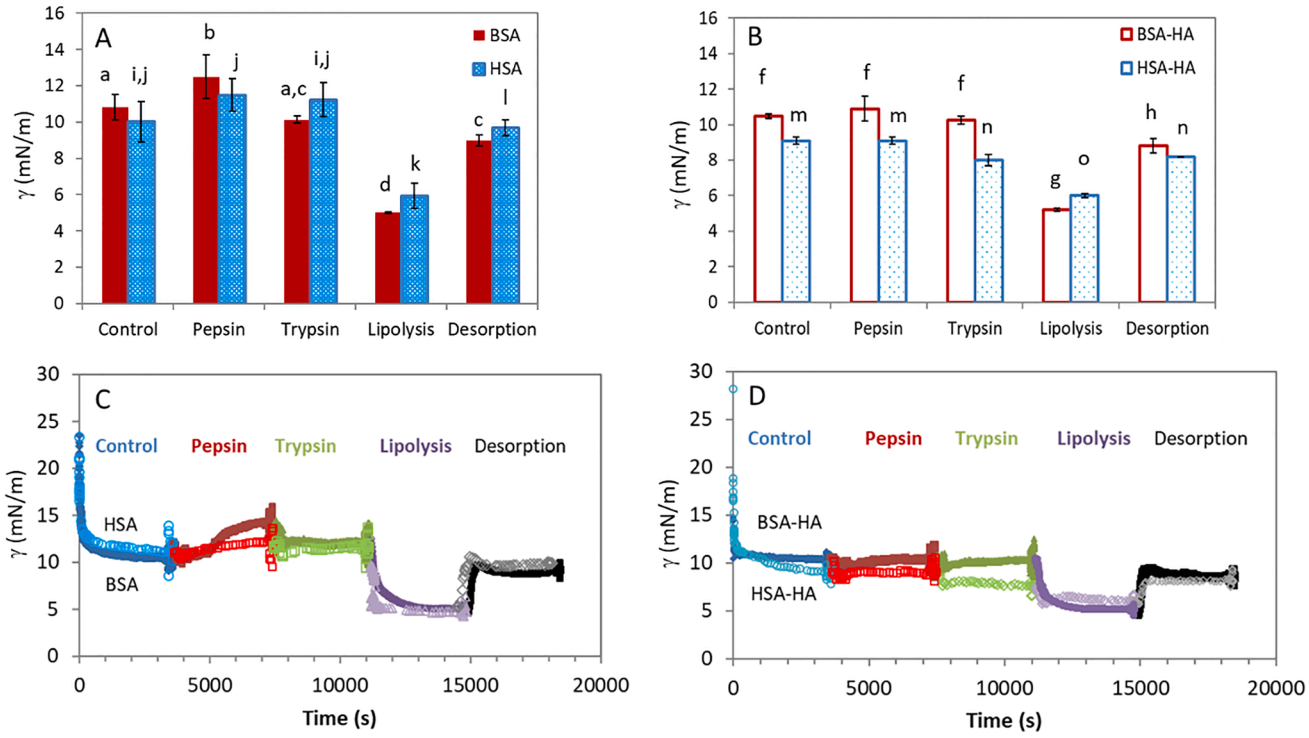

Fig. 4. Final interfacial tension (γ) measured after each phase of the simulated *in vitro* digestion on adsorbed layers at the oil–water interface for (A) BSA (solid red), HSA (solid blue) and (B) BSA + HA (open red), HSA + HA (open blue). The statistic study was made considering the mean value, deviations, and number of repetitions for *in vitro* digestion of each adsorbed layer separately. Different letters (a-l) indicate significant differences between samples ($p < 0.05$). Dynamic evolution of the interfacial tension of *in vitro* digestion of (C) BSA (closed symbols), HSA (open symbols) and (D) BSA + HA (closed symbols), HSA + HA (open symbols) after applying digestive conditions by subphase exchange of the bulk solution with digestive media as described in section 2.1. Concentration of albumins 10^{-5} M and HA $5{\cdot}10^{-7}$ M. Control: phosphate buffer; Pepsin: SGF + pepsin; Trypsin: SIF + trypsin + chymotrypsin; Lipolysis: SIF + Lipase + bile salts; Desorption: SIF. Represented data correspond to one of the performed experiments. (For interpretation of the references to colour in this figure legend, the reader is referred to the web version of this article.)

to desorption of peptides produced by pepsin hydrolysis, diluting the interfacial adsorbed monolayer (Maldonado-Valderrama, 2019). Fig. 4A and 4C show that pepsin hydrolyzes BSA with respect to control BSA layer, whereas HSA resists pepsinolysis as the interfacial tension remains constant during pepsin digestion. It is likely that the less conformational change of HSA upon adsorption provides this improved protection against pepsinolysis (del Castillo-Santaella et al., 2016).

Fig. 4 shows that the presence of HA protects the interfacial BSA from pepsinolysis, as reported in a previous work (Aguilera-Garrido, del Castillo-Santaella, & Galisteo-González et al., 2021). Namely, the interfacial tension remains practically unchanged after pepsin hydrolysis in both cases (Fig. 4B and 4D). It is remarkable that this protective effect of HA proceeds similarly for HSA, suggesting a similar susceptibility to pepsinolysis, of both albumins, in the presence of HA. The polysaccharide HA seems to hinder the enzymatic action, protecting similarly HSA and BSA layers from degradation. Dédinaité and coworkers studied the hydrogen-bonds and hydrophobic interactions between HA and phospholipids in interfacial films. They observed that hydrogen-bond interactions between the polysaccharide and the phospholipids reduced the established hydrogen bonds with water, claiming that phospholipid headgroups can penetrate into certain parts of HA (Dėdinaitė et al., 2019). In a similar way, HA intertwine with albumins, protecting pepsin susceptible sites as it is also shown in Fig. 4. As discussed in section 3.2, the alterations on the ζ-potential of the interacting molecules would reduce the repulsive electrostatic forces between the negatively charged molecules domains at pH 7, allowing the formation of new hydrogen bonds between albumins and HA, thus reinforcing the existing interaction between the molecules and potentially protecting encapsulated material (Dickinson, 2008).

After the gastric phase, the droplet bulk solution is exchanged with sSIF containing trypsin and chymotrypsin enzymes (Fig. 4). Trypsin-chymotrypsin hydrolysis does not seem to have a clear effect on the pepsin-digested-HSA interfacial layer, but significantly reduces the interfacial tension in the case of BSA (Fig. 4A and 4C). The increased resistance of HSA to trypsinolysis could be again related to its limited conformational change at the oil–water interface, which restricts the exposure of enzyme susceptible sites, hence limiting the enzymatic hydrolysis and the digestibility of HSA compared to BSA.

Concerning the effect of HA on trypsinolysis, the interfacial layer formed by BSA + HA remains unaffected by the trypsin step (Fig. 4). The HA provides a similar protective effect against trypsinolysis to BSA but, in the case of HSA + HA, the interfacial tension is slightly reduced (Fig. 4B and 4D). Interestingly, the statistical study shows significant differences between the interfacial tension of BSA + HA and HSA + HA after trypsinolysis, confirming the different digestibility. HA and BSA seem to be interacting and preventing the enzymatic hydrolysis and hence, the degradation of the protein. This different behaviour between BSA + HA and HSA + HA was also previously described in section 3.2, where the interaction of mucin with BSA + HA covered LLNs is more evident than with HSA + HA covered LLNs at pH 7 (Fig. 1). Furthermore, the E measured from mixed and the sequential albumins + HA also showed statistically significant differences between both albumins. All these results suggest that the interaction of HA with BSA and HSA proceeds slightly differently. In the case of BSA + HA, HA is possibly arranged more externally at the LLNs. Hence, this conformation would enable the interaction of BSA + HA LLNs with mucin at pH 7 and protect BSA from enzymatic hydrolysis in the small intestine (pH 7). HSA shows a lower interfacial coverage than BSA (Fig. 2A) and a more rigid interfacial conformation, which may affect the complexation with HA. HA seems to promote interfacial unfolding of HSA, hence the complexation

with HA does not seem to provide a thicker interfacial layer, as the size of the LLNs does not change (Table 1). And it also provides less protection against trypsinolysis as HSA unfolds exposing susceptible sites (Fig. 4B and 4D).

After trypsinolysis, the droplet bulk solution is exchanged with sSIF containing lipase and bile salts. The steep reduction of the interfacial tension within this phase is ascribed to the presence of lipase and bile salts, which are extremely surface-active molecules (del Castillo-Santaella et al., 2014; Maldonado-Valderrama et al., 2013). The experimental results and the statistical study reveal that the interfacial coverage is similar in all cases (Fig. 4).

The different degree of lipolysis can be better evaluated in the final desorption phase, where the droplet bulk solution is exchanged with sSIF. This exchange depletes the bulk solution of hydrophilic products from digestion and bile salts, leaving only lipophilic digestive products at the interface. Thus, the final value of interfacial tension reflects the lipolytic action. Interestingly, HSA interfacial layer provides a significant higher interfacial tension compared to all the other systems (Fig. 4), indicative of less lipolytic action. These are outstanding findings proposing that the limited conformational change of HSA at oil–water interface could provide a slight protective effect against lipolysis, while the presence of HA promotes interfacial unfolding and hence, inhibits or avoids this protective effect (Fig. 4).

In summary, the limited conformational changes of HSA at the oil–water interface seem to provide a further protection against *in vitro* pepsinolysis, trypsinolysis, and lipolysis as compared to BSA. Nevertheless, the presence of HA protects similarly BSA and HSA from *in vitro* pepsinolysis, by hindering the access to pepsin susceptible sites. Conversely, the presence of HA seems to protect BSA against trypsinolysis, but not HSA. This is ascribed to a different arrangement of HA at the interface caused by a different complexation with BSA and HSA. Investigation at the molecular level will provide more details on different complexation sites of BSA and HSA with HA.

4. Conclusions

Serum albumins transport proteins in blood and bind to different kinds of molecules. The different affinity for the same ligand of BSA and HSA can be ascribed to small variations on amino acids sequence despite their similarity in structure and function. BSA-covered LLNs are slightly smaller than HSA-covered LLNs and this relates with an improved emulsifying capacity linked to a higher interfacial coverage reached by BSA (lower interfacial tension). The interfacial characterization provides experimental evidence of a limited conformation change undergone by HSA respect to BSA adsorbed layers at the oil–water interface. BSA + HA and HSA + HA-LLNs display all similar sizes indicative of similar interfacial coverage, as corroborated by interfacial tension and dilatational elasticity. All LLNs are stabilised by electrostatic repulsion at pH 7. The presence of HA clearly promotes the hydrophobic interaction of LLNs with mucins, being this effect more notable at pH 3 where the reduction of the electrostatic repulsion between mucin and albumins promotes the formation of hydrogen bonding. At pH 7 only the interaction of mucins and BSA + HA covered LLNs is measurable. Further differences between HSA and BSA adsorbed films arise when looking into the interaction with digestive media in the absence and presence of HA. The presence of HA protects similarly BSA and HSA from *in vitro* pepsinolysis, while HSA + HA is more susceptible to trypsin hydrolysis owing to the unfolding induced in HSA by complexation with HA. Ultimately, the limited conformational changes of HSA provide the largest protection against *in vitro* trypsinolysis and lipolysis. BSA is a common model protein widely used, but HSA is more relevant from a clinical view. The differences highlighted in this work regarding interaction with HA and digestibility should be considered in the design of LLNs for oral delivery systems.

CRediT authorship contribution statement

Teresa del Castillo-Santaella: Methodology, Validation, Formal analysis, Investigation, Visualization, Writing – original draft. **Aixa Aguilera-Garrido:** Methodology, Validation, Formal analysis, Investigation, Visualization, Writing – original draft. **Francisco Galisteo-González:** Conceptualization, Writing – review & editing, Supervision, Project administration. **María José Gálvez-Ruiz:** Writing – review & editing, Supervision, Project administration, Funding acquisition. **José Antonio Molina-Bolívar:** Methodology, Investigation, Writing – original draft. **Julia Maldonado-Valderrama:** Conceptualization, Writing – review & editing, Supervision.

Declaration of Competing Interest

The authors declare that they have no known competing financial interests or personal relationships that could have appeared to influence the work reported in this paper.

Acknowledgements

This work has been supported by project RTI2018-101309-B-C21 funded by MCIN/AEI/10.13039/501100011033/FEDER. The authors are also grateful to the “Mancomunidad de los Pueblos de la Alpujarra Granadina” for the funds raised and supplied for this research by “Solidaridad entre montañas” project. This work was also partially supported by the Biocolloid and Fluid Physics Group (ref. PAI-FQM115) of the University of Granada (Spain). JMV acknowledges support from project Project PID2020-116615RA-I00 funded by MCIN/ AEI /10.13039/501100011033. This work has been done in the framework of the doctorate of AAG in the Doctoral Programme in Biomedicine (B11/56/1) of the University of Granada. Funding for open access charge: Universidad de Granada / CBUA.

References

Aguilera-Garrido, A., del Castillo-Santaella, T., Galisteo-González, F., Gálvez-Ruiz, M. J., & Maldonado-Valderrama, J. (2021). Investigating the role of hyaluronic acid in improving curcumin bioaccessibility from nanoemulsions. *Food Chemistry, 351*, Article 129301. https://doi.org/10.1016/j.foodchem.2021.129301

Aguilera-Garrido, A., del Castillo-Santaella, T., Yang, Y., Galisteo-González, F., Gálvez-Ruiz, M. J., Molina-Bolívar, J. A., … Maldonado-Valderrama, J. (2021). Applications of serum albumins in delivery systems: Differences in interfacial behaviour and interacting abilities with polysaccharides. *Advances in Colloid and Interface Science, 4* (5), 932–942. https://doi.org/10.1016/j.cis.2021.102365

Aguilera-Garrido, A., Molina-Bolívar, J. A., Gálvez-Ruiz, M. J., & Galisteo-González, F. (2019). Mucoadhesive properties of liquid lipid nanocapsules enhanced by hyaluronic acid. *Journal of Molecular Liquids, 296*, 102365. https://doi.org/10.1016/j.molliq.2019.111965

Akiyama, E., Kashimoto, A., Fukuda, K., Hotta, H., Suzuki, T., & Kitsuki, T. (2005). Thickening properties and emulsification mechanisms of new derivatives of polysaccharides in aqueous solution. *Journal of Colloid and Interface Science, 282*(2), 448–457. https://doi.org/10.1016/j.jcis.2004.08.178

Baeza, R., Pilosof, A. M. R., Sánchez, C. C., & Rodríguez Patino, J. M. (2006). Adsorption and rheological properties of biopolymers at the air-water interface. *AIChE Journal, 52*(7), 2627–2638. https://doi.org/10.1002/aic.10855

Chen, S., Han, Y., Wang, Y., Yang, X., Sun, C., Mao, L., & Gao, Y. (2019). Zein-hyaluronic acid binary complex as a delivery vehicle of quercetagetin: Fabrication, structural characterization, physicochemical stability and in vitro release property. *Food Chemistry, 276*, 322–332. https://doi.org/10.1016/J.FOODCHEM.2018.10.034

Day, L., Zhai, J., Xu, M., Jones, N. C., Hoffmann, S. V., & Wooster, T. J. (2014). Conformational changes of globular proteins adsorbed at oil-in-water emulsion interfaces examined by synchrotron radiation circular dichroism. *Food Hydrocolloids, 34*, 78–87. https://doi.org/10.1016/j.foodhyd.2012.12.015

de Oliveira Cardoso, V. M., Gremião, M. P. D., & Cury, B. S. F. (2020). Mucin-polysaccharide interactions: A rheological approach to evaluate the effect of pH on the mucoadhesive properties. *International Journal of Biological Macromolecules, 149*, 234–245. https://doi.org/10.1016/j.ijbiomac.2020.01.235

Dėdinaitė, A., Wieland, D. C. F., Bełdowski, P., & Claesson, P. M. (2019). Biolubrication synergy: Hyaluronan – Phospholipid interactions at interfaces. *Advances in Colloid and Interface Science, 274*, 1–12. https://doi.org/10.1016/j.cis.2019.102050

del Castillo-Santaella, T., Maldonado-Valderrama, J., Molina-Bolivar, J. A., & Galisteo-Gonzalez, F. (2016). Effect of cross-linker glutaraldehyde on gastric digestion of emulsified albumin. *Colloids and Surfaces B: Biointerfaces, 145*, 899–905. https://doi.org/10.1016/j.colsurfb.2016.06.014

del Castillo-Santaella, T., Sanmartin, E., Cabrerizo-Vílchez, M. A., Arboleya, J. C., & Maldonado-Valderrama, J. (2014). Improved digestibility of β-lactoglobulin by pulsed light processing: A dilatational and shear study. *Soft Matter, 9702–9714*. https://doi.org/10.1039/C4SM01667J

Dickinson, E. (2008). Interfacial structure and stability of food emulsions as affected by protein–polysaccharide interactions. *Soft Matter, 4*(5), 932–942. https://doi.org/10.1039/B718319D

Douillard, R. (1994). Adsorption of serum albumin at the oil / water interface. *Colloids and Surfaces, 91*, 113–119. https://doi.org/10.1016/0927-7757(94)02764-1

Fallacara, A., Baldini, E., Manfredini, S., & Vertuani, S. (2018). Hyaluronic acid in the third millennium. *Polymers, 10*(7), 701. https://doi.org/10.3390/polym10070701

Galisteo-González, F., Molina-Bolívar, J. A., Navarro, S. A., Boulaiz, H., Aguilera-Garrido, A., Ramírez, A., & Marchal, J. A. (2018). Albumin-covered lipid nanocapsules exhibit enhanced uptake performance by breast-tumor cells. *Colloids and Surfaces B: Biointerfaces, 165*, 103–110. https://doi.org/10.1016/j.colsurfb.2018.02.024

Hansen, I. M., Ebbesen, M. F., Kaspersen, L., Thomsen, T., Bienk, K., Cai, Y., … Howard, K. A. (2017). Hyaluronic acid molecular weight-dependent modulation of mucin nanostructure for potential mucosal therapeutic applications. *Molecular Pharmaceutics, 14*(7), 2359–2367. https://doi.org/10.1021/acs.molpharmaceut.7b00236

Kim, S., & Shin, W. S. (2021). Formation of a novel coating material containing lutein and zeaxanthin via a Maillard reaction between bovine serum albumin and fucoidan. *Food Chemistry, 343*, Article 128437. https://doi.org/10.1016/J.FOODCHEM.2020.128437

Li, R., Ng, T. S. C., Wang, S. J., Prytyskach, M., Rodell, C. B., Mikula, H., … Miller, M. A. (2021). Therapeutically reprogrammed nutrient signalling enhances nanoparticulate albumin bound drug uptake and efficacy in KRAS-mutant cancer. *Nature Nanotechnology, 16*, 830–839. https://doi.org/10.1038/s41565-021-00897-1

List, S. J., Findlay, B. P., Forstner, G. G., & Forstner, J. F. (1978). Enhancement of the viscosity of mucin by serum albumin. *Biochemical Journal, 175*(2), 565–571. https://doi.org/10.1042/bj1750565

Lorenzo, G., Zaritzky, N., & Califano, A. (2013). Rheological analysis of emulsion-filled gels based on high acyl gellan gum. *Food Hydrocolloids, 30*(2), 672–680. https://doi.org/10.1016/j.foodhyd.2012.08.014

Lu, J. R., Su, T. J., & Penfold, J. (1999). Adsorption of Serum Albumins at the Air/Water Interface. *Langmuir, 15*(20), 6975–6983. https://doi.org/10.1021/la990131h

Luo, R., Lin, M., Zhang, C., Shi, J., Zhang, S., Chen, Q., … Gao, F. (2020). Genipin-crosslinked human serum albumin coating using a tannic acid layer for enhanced oral administration of curcumin in the treatment of ulcerative colitis. *Food Chemistry, 330*, 127241. https://doi.org/10.1016/J.FOODCHEM.2020.127241

Ma, G. J., Ferhan, A. R., Sut, T. N., Jackman, J. A., & Cho, N. J. (2020). Understanding how natural sequence variation in serum albumin proteins affects conformational stability and protein adsorption. Colloids and Surfaces B: Biointerfaces, 194(March), 111194. https://doi.org/10.1016/j.colsurfb.2020.111194.

Maldonado-Valderrama, J. (2019). Probing in vitro digestion at oil–water interfaces. *Current Opinion in Colloid and Interface Science, 39*, 51–60. https://doi.org/10.1016/j.cocis.2019.01.004

Maldonado-Valderrama, J., Holgado-Terriza, J. A., Torcello-Gómez, A., & Cabrerizo-Vílchez, M. A. (2013). In vitro digestion of interfacial protein structures. *Soft Matter*, 1043–1053. https://doi.org/10.1039/c2sm26843d

Maldonado-Valderrama, J., Muros-Cobos, J. L., Holgado-Terriza, J. A., & Cabrerizo-Vílchez, M.Á. (2014). Bile salts at the air-water interface: Adsorption and desorption. *Colloids and Surfaces B: Biointerfaces, 120*, 176–183. https://doi.org/10.1016/j.colsurfb.2014.05.014

Maldonado-Valderrama, J., Torcello-Gómez, A., del Castillo-Santaella, T., Holgado-Terriza, J. A., & Cabrerizo-Vílchez, M. A. (2015). Subphase exchange experiments with the pendant drop technique. *Advances in Colloid and Interface Science, 222*. https://doi.org/10.1016/j.cis.2014.08.002

Minekus, M., Alminger, M., Alvito, P., Ballance, S., Bohn, T., Bourlieu, C., … Brodkorb, A. (2014). A standardised static in vitro digestion method suitable for food - an international consensus. *Food & Function, 5*(6), 1113–1124. https://doi.org/10.1039/c3fo60702j

Moore, J., & Cerasoli, E. (2017). Particle Light Scattering Methods and Applications. In *Encyclopedia of Spectroscopy and Spectrometry* (Third Edition, pp. 543–553). Elsevier.

Murray, B. S. (2011). Rheological properties of protein films. *Current Opinion in Colloid & Interface Science, 16*(1), 27–35. https://doi.org/10.1016/j.cocis.2010.06.005

Pan, Y., Xie, Q. T., Zhu, J., Li, X. M., Meng, R., Zhang, B., … Jin, Z. Y. (2019). Study on the fabrication and in vitro digestion behavior of curcumin-loaded emulsions stabilized by succinylated whey protein hydrolysates. *Food Chemistry, 287*, 76–84. https://doi.org/10.1016/J.FOODCHEM.2019.02.047

Petrou, G., & Crouzier, T. (2018). Mucins as multifunctional building blocks of biomaterials. *Biomaterials Science, 6*(9), 2282–2297. https://doi.org/10.1039/c8bm00471d

Plaza-Oliver, M., Santander-Ortega, M. J., Castro-Vázquez, L., Rodríguez-Robledo, V., González-Fuentes, J., Marcos, P., … Arroyo-Jiménez, M. M. (2020). The role of the intestinal-protein corona on the mucodiffusion behaviour of new nanoemulsions stabilised by ascorbyl derivatives. *Colloids and Surfaces B: Biointerfaces, 186*, Article 110740. https://doi.org/10.1016/j.colsurfb.2019.110740

Radicioni, G., Cao, R., Carpenter, J., Ford, A. A., Wang, T. T., Li, Y., & Kesimer, M. (2016). The innate immune properties of airway mucosal surfaces are regulated by dynamic interactions between mucins and interacting proteins: The mucin interactome. *Mucosal Immunology, 9*(6), 1442–1454. https://doi.org/10.1038/mi.2016.27

Rodríguez Patino, & Pilosof, A. M. R. (2011). Protein-polysaccharide interactions at fluid interfaces. *Food Hydrocolloids, 25*(8), 1925–1937. https://doi.org/10.1016/j.foodhyd.2011.02.023

Uspenskii, S. A., Kil'deeva, N. R., Maslova, M.v., Demina, T. S., & Vikhoreva, G. A. (2016). A study of the viscosity of hyaluronic acid solutions for the preparation of polyelectrolyte complexes with chitosan. *Russian Chemical Bulletin, 65*(1), 273–276. https://doi.org/10.1007/s11172-016-1296-0

Wagner, C. E., Wheeler, K. M., & Ribbeck, K. (2018). Mucins and Their Role in Shaping the Functions of Mucus Barriers. *Annual Review of Cell and Developmental Biology, 34*(1), 189–215. https://doi.org/10.1146/annurev-cellbio-100617-062818

Wang, Y. Y., Lai, S. K., Suk, J. S., Pace, A., Cone, R., & Hanes, J. (2008). Addressing the PEG mucoadhesivity paradox to engineer nanoparticles that "slip" through the human mucus barrier. *Angewandte Chemie - International Edition, 47*(50), 9726–9729. https://doi.org/10.1002/anie.200803526

Yakubov, G. E., Papagiannopoulos, A., Rat, E., & Waigh, T. A. (2007). Charge and interfacial behavior of short side-chain heavily glycosylated porcine stomach mucin. *Biomacromolecules, 8*(12), 3791–3799. https://doi.org/10.1021/bm700721c

Yu, H., & Huang, Q. (2010). Enhanced in vitro anti-cancer activity of curcumin encapsulated in hydrophobically modified starch. *Food Chemistry, 119*(2), 669–674. https://doi.org/10.1016/J.FOODCHEM.2009.07.018